Morphology and Alignment of Volcanic Vents:

Puna Plateau, NW Argentina

Senior Thesis

Presented in Partial Fulfillment of the Requirements for a Bachelor of Sciences Degree at the Ohio State University

By John Patrick Calhoun

*****

The Ohio State University

2010

Approved by

_____.

Lindsay Schoenbohm, Advisor
School of Earth Sciences

Introduction

Morphology and alignment of monogenetic cinder cones and locations of flows can provide useful information about contemporary and past tectonic stress directions. This derivation of stress direction requires that the study sites are well preserved and/or relatively young (~7 Ma) in age, do not show radial patterns around a polygenetic volcano as is typical for isotropic stress fields, and are not controlled by local factors such as volcano topography, magma chamber shape and pressures, or surface loading (Nakamura, 1977; Paulsen and Wilson, 2010).

The Altiplano-Puna plateau of NW Argentina contains many volcanic features and within the southern Puna there is an abundance of young mafic monogenetic cinder cones. These cones are excellent indicators of stress and hold crucial information about the state of tectonic stresses during eruption. Within the back-arc section in the Puna plateau is a distinct style of volcanism composed of small volume mafic cones and fissure flows ranging in composition from basalt to dacite (Kay et al., 1994; Kramer et al., 1999; Risse et al., 2008). The focus area of this study, the southern Puna, is geographically characterized by fault-bounded ranges and intervening, high elevation basins (Allmendinger et al., 1997; Coutand et al., 2001). Both recent and past research has provided remarkable insight into the relatively poorly understood processes of continental plateau evolution; this study aims to further that knowledge by providing morphologic data on 48 late Miocene-Recent (~7 Ma) small mafic monogenetic volcanoes from the southern Puna Plateau (~25°-27° S). We provide new data on cone location, morphology, and vent alignment, and discuss identification and evaluation of local and regional stresses using alignment/morphometric data to determine if our data support or contradict structural data from faults, and to test between proposed models of lithospheric thinning.

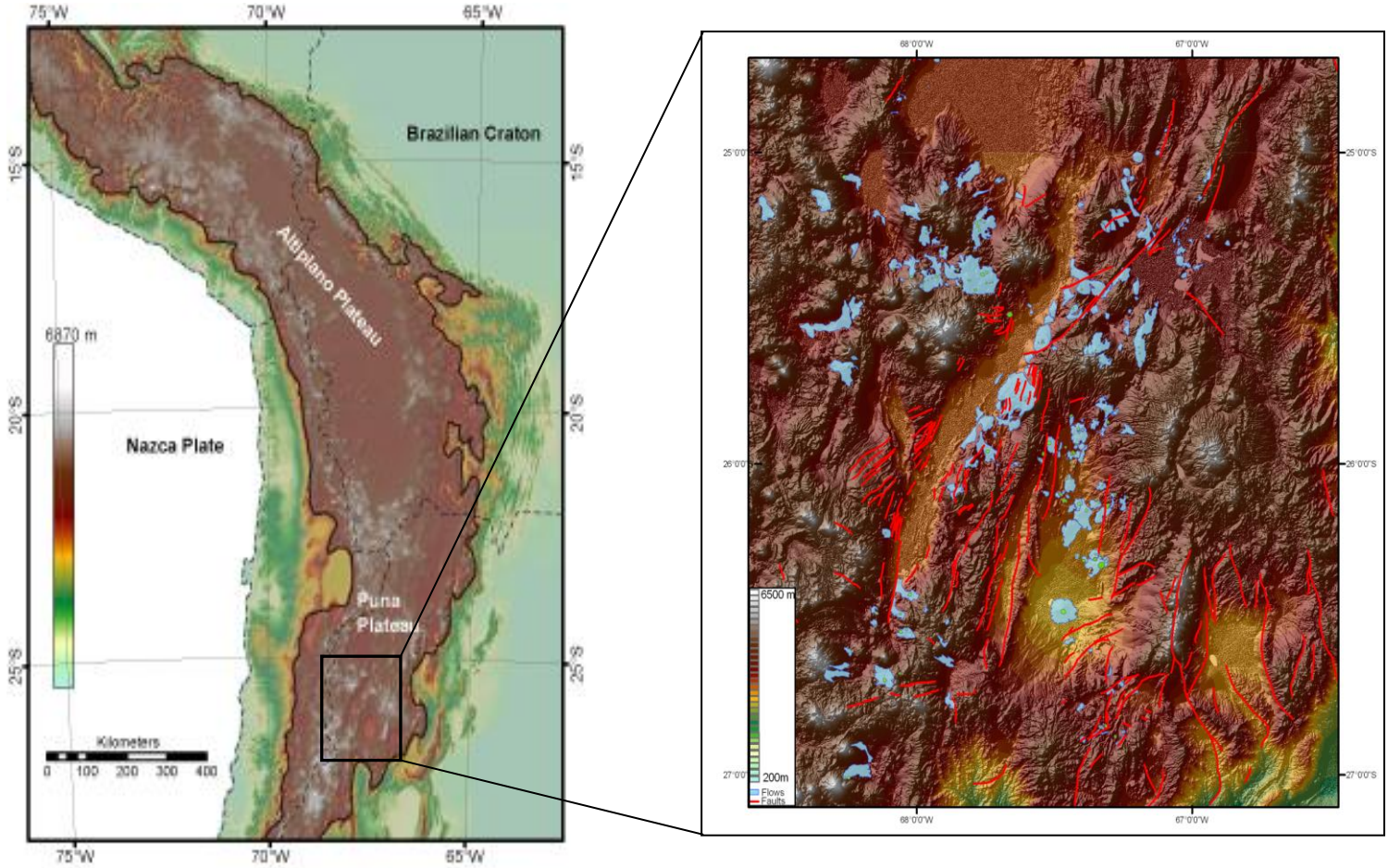

Figure 1. The Altiplano-Puna Plateau. Faults (red) are seen to run NNE-SSW generally. Volcanoes (blue) are scattered about the plateau

Geologic setting

Tectonic Setting

The Puna-Altiplano Plateau of NW Argentina (figure 1) is the second largest plateau found on Earth, and the largest plateau formed from oceanic-continental plate convergence. The entire plateau is defined by the area above 3 km stretching 1800 km along the backbone of the Andes, from southern Peru to northern Argentina. It varies between 350 and 400 km in width, with peaks extending over 6.8 km (Isacks, 1988; Allmendinger et al., 1997 and references therein). The tectonic history of the plateau is

broadly understood as evolving by means of subduction of the oceanic Nazca plate beneath the South American plate which led to extensive horizontal shortening and vertical extension (thickening) of the over-riding South American plate (Allmendinger et al., 1997). Complementary models describe a link between magmatism and lithospheric delamination which could have contributed to the plateau growth (Kay et al., 1994; Beck and Zandt, 2002; Grazione et al., 2006). The Western Cordillera has experienced subduction related arc-volcanism in the form of large stratovolcano complexes, and from 16-12 Ma, the Puna back-arc has experienced abundant andesitic and dacitic eruptions (Allmendinger et al., 1997).

The southern Puna is characterized by a hyper-arid climate. Fault-bounded N-S to NE-SW trending mountain ranges separate high elevation internally drained basins and salars (salt flats) which cover considerable areas of 1000-1800 km² (Allmendinger et al., 1997). Crustal thickness beneath the Puna is 50-55 km on average, as opposed to 75 km beneath the Altiplano and is thought to be mostly intermediate to felsic in composition (Drew et al., 2009 and references therein). Total lithospheric thickness is only 60 km which suggests a relatively thin (5-10 km) mantle lithosphere (Tassara et al., 2006). This value is considerably less than expected considering the amount of shortening (>150km) evidenced in the upper crust (Kley and Monaldi, 1998).

Miocene-Pliocene deformation on the Puna consists of thrust faults that have accommodated NW-SE shortening and vertical extension (Allmendinger et al., 1989; Marrett et al., 1994). This compressional regime is active today around the margins of the plateau (Schoenbohm and Strecker 2009). Simultaneously at high elevations, normal and strike-slip faults accommodate NE-SW to N-S extension since at least quaternary time (Allmendinger et al., 1989; Marrett et al., 1994). Some of this recent extension is believed to have been accommodated through exploitation of inherited thrust planes,

resulting in an overprinting of extensional tectonics on compressional tectonics (Schoenbohm and Strecker, 2009 and references therein). These extensional faults may reflect the increase in gravitational potential energy accompanying detachment of foundering lithosphere, but could also reflect an incipient gravitational extensional collapse of the plateau as a whole (Schoenbohm and Strecker, 2009).

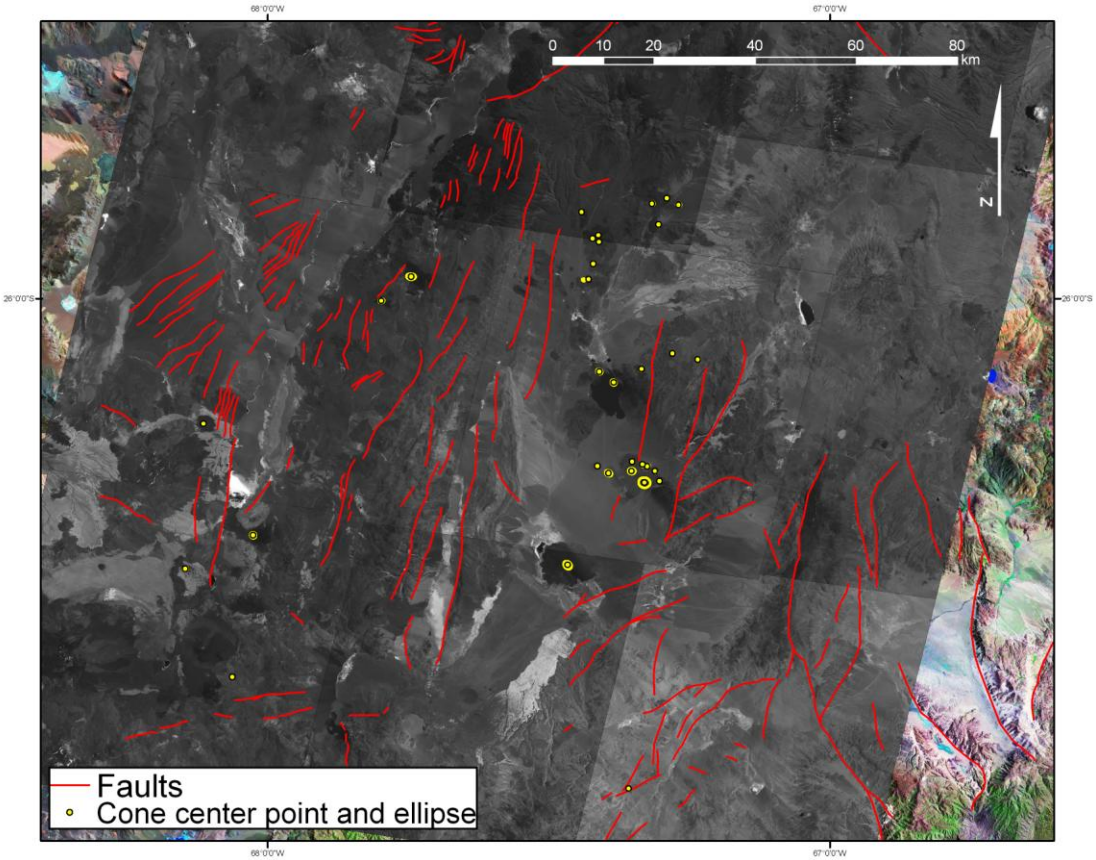

Figure 2. Faults are mapped in red and show a strong preferred surface trend to the NE-SW. Faults mapped by L. Schoenbohm.

Volcanic Setting

Volcanism in the Andes is characterized by large arc-related stratovolcano complexes coinciding temporally with compression in the region (Allmendinger et al., 1997). The Puna Ojos del Salado (27.1°S, 6887 m elev.) and Lullaillaco (24.7°S, 6723 m elev.) complexes are the highest active volcanic centers on Earth (Allmendinger et al., 1997). These orogen parallel complexes are composed primarily of andesitic to dacitic

lavas, domes and pyroclastic flows. The Altiplano-Puna volcanic complex (APVC) is the world's largest young continental volcanic field, covering an area of at least 50,000 km² in the southern Altiplano and northern Puna plateaus. It is composed of large calc-alkaline ignimbrite centers (de Silva, 1989; Drew et al,. 2009). The APVC is present in the Puna in the form of widespread andesitic and dacitic eruptions from 16-12 Ma, temporally coincident with uplift in the southern Puna Plateau (Coira et al., 1993). Younger eruptions of large-volume ignimbrites from late Miocene to Pliocene time are believed to be the result of extensive crustal melting caused by the presence of mantle-derived magmas (Francis et al., 1989; Coira et al., 1993).

The southern Puna contains many small mafic monogenetic cones and fissure flows of late Miocene (~7 Ma) to recent age. These basaltic to andesitic magmas are most voluminous in the southern Puna and are dominantly mantle-derived (Allmendinger et al., 1997). This mafic volcanism is typified by monogenetic to simple polygenetic cinder cones and lava flows which cover areas less than a few km². Dating of these lavas has provided ages indicative of eruption after 3.5 Ma for most of the lavas in the southern and central Puna but some date back to 7.3 Ma (Risse et al., 2008). These cinder cones may or may not have an associated lava flow and likewise some of the flows have cannibalized their cones leaving only broad, flat, expansive flows. These young centers in the southern Puna are related to extensional dip slip or strike-slip along generally N-S trending faults (Marrett and Emerman, 1992; Marrett et al., 1994). Some of the younger, mafic flows have been shown to have intraplate-like geochemical signatures which may point to lithospheric delamination beneath the Puna plateau (Kay et al., 1994).

In the Western Cordillera, volcanic activity has been nearly continuous from the Miocene to the Holocene. In the Altiplano-Puna plateau, two volcanic styles which differ in their spatial and temporal distribution can be distinguished: (a) Middle-Upper Miocene

volcanism related to major transverse (NW-SE) lineaments; and (b) Pliocene-Quaternary, mainly monogenetic volcanic centers developed principally in the southern Puna plateau. Trans-arc volcanism along the NW-SE lineaments has been related to variations in the dip of the subducting Nazca plate (Kay et al., 1999; Matteini et al., 2002).

Lithospheric Foundering

Lithospheric foundering is the sinking of a mantle lithosphere and potentially lower continental crust into the asthenosphere. This is a result of density contrasts between thickened cold, dense lithospheric mantle/lowermost crust and the underlying hot, less dense asthenosphere (Kay and Kay, 1993). During lithospheric foundering, the hot, less dense asthenosphere rises it replaces the cold, denser lithosphere (Kay and Kay 1993; Schott and Schmeling, 1998). The thickening necessary to promote lithospheric foundering is driven by crustal shortening in continental settings caused by compressional tectonics. Along with crustal thickening, the density contrasts mentioned above can also contribute to the lithospheric foundering process. Crustal thickening is believed to be a precursor to extensional tectonics in compressional settings (Dewey 1988).

Kay and Kay (1993) and Kay et al (1994) argue that lithospheric foundering may be related to crustal extension and magmatism in the Puna Plateau. Allmenginger (1986) show that the stress regime in the southern Puna underwent a noticeable change from compression to extension and Kay (1994) and Risse (2008) argue for the spatial and temporal correlation of this transition with the onset of mafic volcanism in the region. Recent research by Schoenbohm and Strecker (2009) argues that extension is more spatially and temporally diverse than required by the lithospheric foundering model

proposed by Kay and Kay (1993). Proposed models for lithospheric foundering include delamination, full convective removal, partial convective removal, and piecemeal removal (Gogus and Pysklywec, 2008; Carrapa et al., 2009). Delamination is a simple 'peeling back' of the lithosphere along a detachment between the crust and mantle lithosphere. Full convective removal describes a large lithospheric drip which fully removes the lithosphere as hotter asthenosphere rises to replace it via convection beneath the southern Puna plateau. Partial convective removal is similar to full convective removal except that part of the mantle lithosphere is left intact. Piecemeal removal occurs through many small lithospheric drips.

These models would all produce different stress fields in the crust; delamination would predict a sweep of deformation across the plateau, following the progress of the delaminating lithospheric slab. Partial or full convective removal would predict a radial or concentric deformation field. Piecemeal foundering would predict complicated temporal extension patterns. This effect, however, may be overwhelmed by extensional strain related to gravitational extensional collapse or back-arc extension within the plateau, which could produce more uniform NW-SE extension.

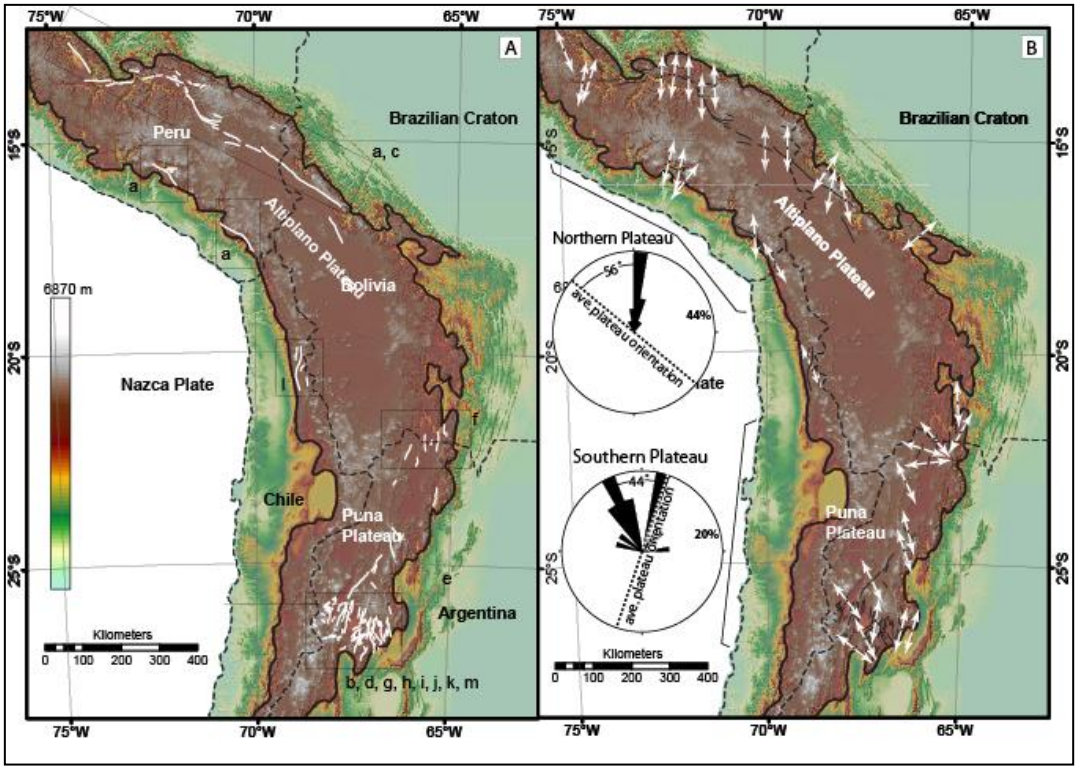

Figure 3. from Schoenbohm et.al., 2009(figure 10) highlighting two different extensional directions in the southern Puna plateau as indicated by extensional strike-slip faults. Inset rose diagrams show extension directions.

Methodology and Data Collection

Field Relationships

48 volcanic cinder cones were mapped remotely using ASTER satellite imagery and digital elevation models (DEM) in ArcGIS to determine the location, type, and morphology of volcanic edifices as well as their relationship with previously mapped faults. Precise GPS locations of many of the cones and flows were mapped in the field. This mapping reveals a variety of settings including isolated volcanoes with no apparent relationship to surface faulting, volcanoes and flows situated along or near surface faults, and clusters or fields of volcanoes, some of which lie along or near faults.

Cinder Cone Morphology

Morphometric attributes of volcanic vents such as basal or crater elongation, is directly related to the trend of subsurface fissures that control alignments (Nakamura, 1977; Tibaldi, 1995; Paulsen and Wilson, 2010). Elongated vents therefore are critical for defining reliable regional vent alignments, and also provide an independent means for assessing stress directions (Paulsen and Wilson, 2010).

The "Directional Distribution: Standard Deviational Ellipse" tool in ArcGIS was used to construct best-fit ellipses around the bases of 48 cones on the southern Puna Plateau. This tool provides lengths of major and minor axes of each ellipse, the orientation of the long axis, and the center point of the ellipse. These statistics (see appendix 1) allowed for alignment analysis in two locations where clusters of cones and flows occur; the Jote field, which contains two possible alignments, and the Nacimientos field.

Volcano Distribution and Alignment

The methods put forth by Nakamura (1977) were applied in conjunction with more recently published methods by Paulsen and Wilson (2010) to determine the fracture and fault geometry for both individual volcanoes and clusters. The pattern of volcanoes and their subsurface feeder dikes reflects the regional non-magmatic stress superposed on the magmatic pressure (Nakamura, 1977). These stresses influence the eruptive style of volcanoes and indicate that eruption along a strike-slip fault will tend to breach parallel to the trend of the fault, while those erupted along dip-slip faults will tend to breach perpendicular to fault trend (Tibaldi, 1995).

In general, large, conduit-fed, polygenetic volcanoes tend to align perpendicular to maximum horizontal stress in compressional settings, while monogenetic fracture-fed volcanoes will align parallel to maximum horizontal compressional stress. In an

extensional regime, however, both styles of volcanism will align perpendicular to direction of maximum horizontal extension. For volcanic fields consisting of clusters of monogenetic volcanoes, the average strike of eruptive fissures and alignment of monogenetic craters are taken as the surface expression of the dike trends (Nakamura, 1977).

Paulsen and Wilson (2010) have built on the conceptual framework of Nakamura and others and introduced parameters aimed at classifying the reliability of vent alignments, which provides a methodology for vent mapping. The parameters are meant to assess the confidence with which proposed alignments reflect subsurface dike trends. These methods are generally applicable to identifying structure and the stress field by assuming that volcanoes are points (x,y) with trends that delineate underlying fractures and/or faults.

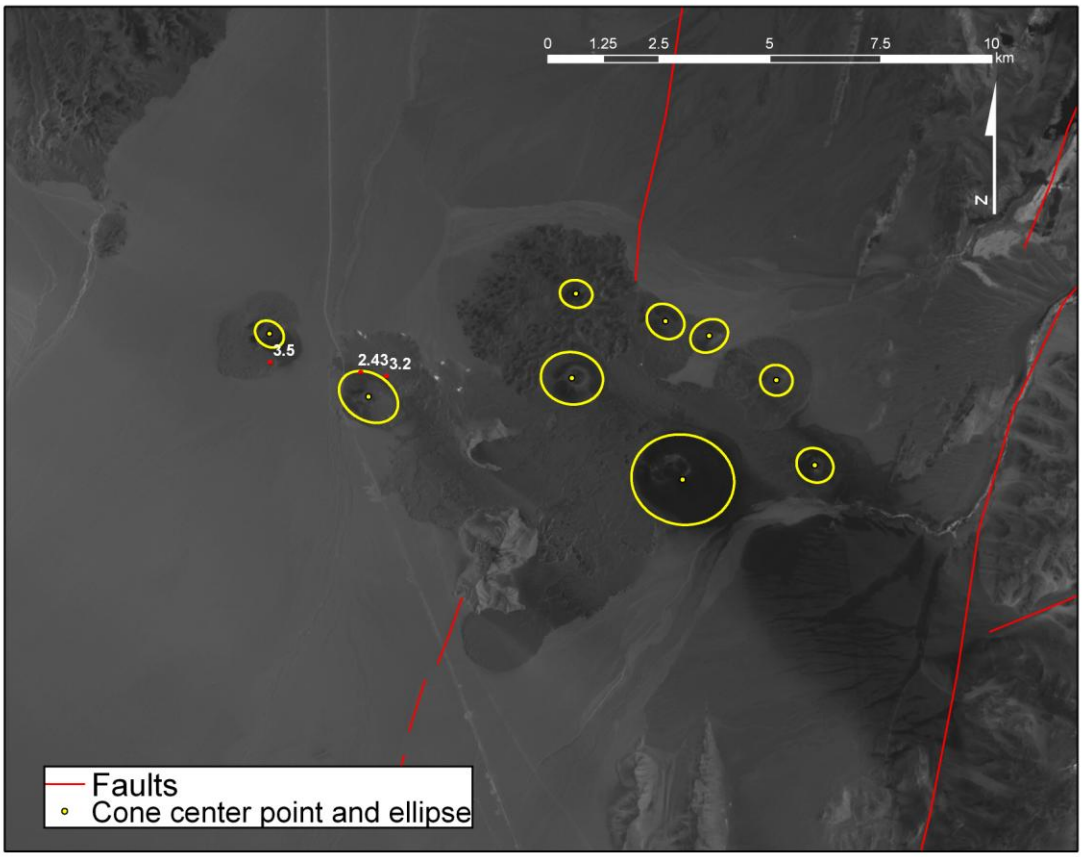

Figure 4. Showing ellipses fitted to the bases of vents within the Jote field. Published ages in Ma (Risse et al,. 2008).

Alignment analysis within these two fields is based on the parameters put forth by Paulsen and Wilson (2010); (1) the number of vents in each field, (2) the length of alignment defined as the distance between the two end vents, (3) the standard deviation of the vent centers from a best fit line through the cluster, (4) the number of elongate vents (>1.2 ratio between the lengths of the long and short axes) in the field, (5) the standard deviation of the trends of elongate vent axes from that of the best fit line, and (6) the average spacing between vents within the fields.

Once mapped, the ellipse center points in each field were used to construct a best fit line, the axial data were used to calculate all above mentioned parameters, and reliability assessment grades were assigned (see Table 1). Parameter (4) above is based on the axial ratios of the vents where ratios <1.2 are classified as circular, ≥1.2 and <1.4 as slightly elongate, ≥1.4 and <1.6 as elongate, ≥1.6 and <1.8 as very elongate, and ≥1.8 as cleft cones (Paulsen and Wilson, 2010).

Results

Regional

The 48 vents that were measured and analyzed across the southern Puna Plateau show a preferred long-axis orientation toward the NW-SE (N120W) (Figure 5.). Of the vents that were measured; 27 were circular, 18 were slightly elongate, 1 was elongate, and one was a cleft cone, which Paulsen and Wilson (2010) classify as having a trend highly indicative of subsurface fissures. Most of the available regional fault data show faults striking NNE-SSW, which is nearly perpendicular to average cone elongation.

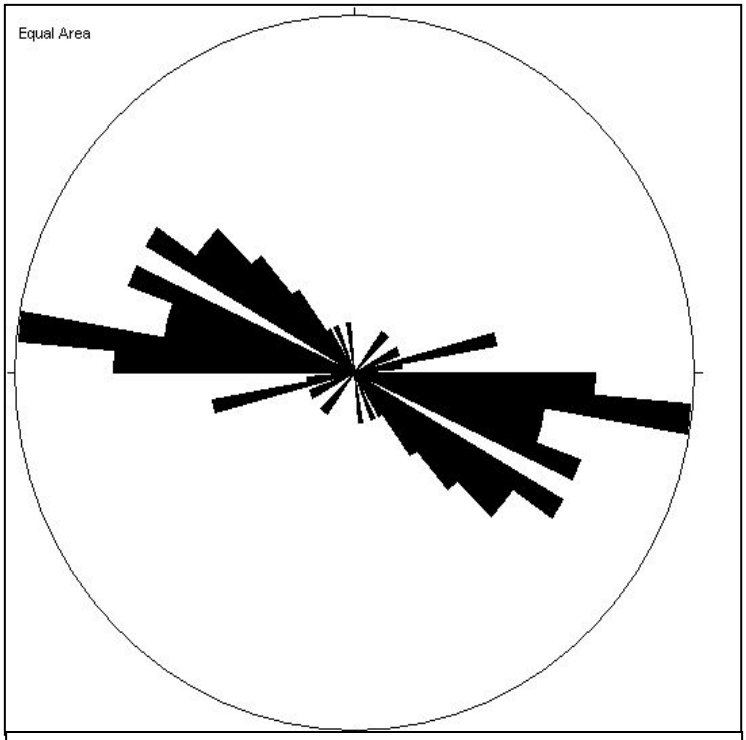

Figure 5. Rose diagram showing long axis azimuths of 48 ellipses measured in the southern Puna Plateau.

Nacimientos Volcanic Field

The Nacimientos area, located just north of the Antofagasta basin, contains many NNE-SSW trending faults, some of which appear to have flows associated with them. The cluster I focused on contains 7 vents with an average spacing distance of 1592 m and an average long axis azimuth of 120° (36°, 110°, 125°, 166°, 105°, 176°) Of these cones, only one is considered "elongate" and is actually a cleft cone. The breaching directions of these vents are dominantly westward with two breaching ~310°, two at ~ 245° and 270°, and one cleft cone which breached to the north and south, expelling much more lava to the south toward ~ 180°. A reactivated, oblique-slip fault striking NNE-SSW accommodating relatively N-S extension has been inferred in the area of the Nacimientos field. The ractivated fault strike closely matches the volcano alignment. According to the reliability assessment grading (Table 2) of Paulsen and Wilson (2010),

the Nacimientos alignment achieves a grade of “A” for three of the four applicable categories (# of vents, index of vent elongation, and standard angular deviation vent long axes), and a “C” in the fourth category of standard deviation best fit line distance. The structure of their system calls for the lowest grade achieved within one field to represent the field as a whole, resulting in an overall “C” grade. However, one could argue that the average grade that the alignment achieves would prove a higher level of confidence in its reflection of subsurface geometry.

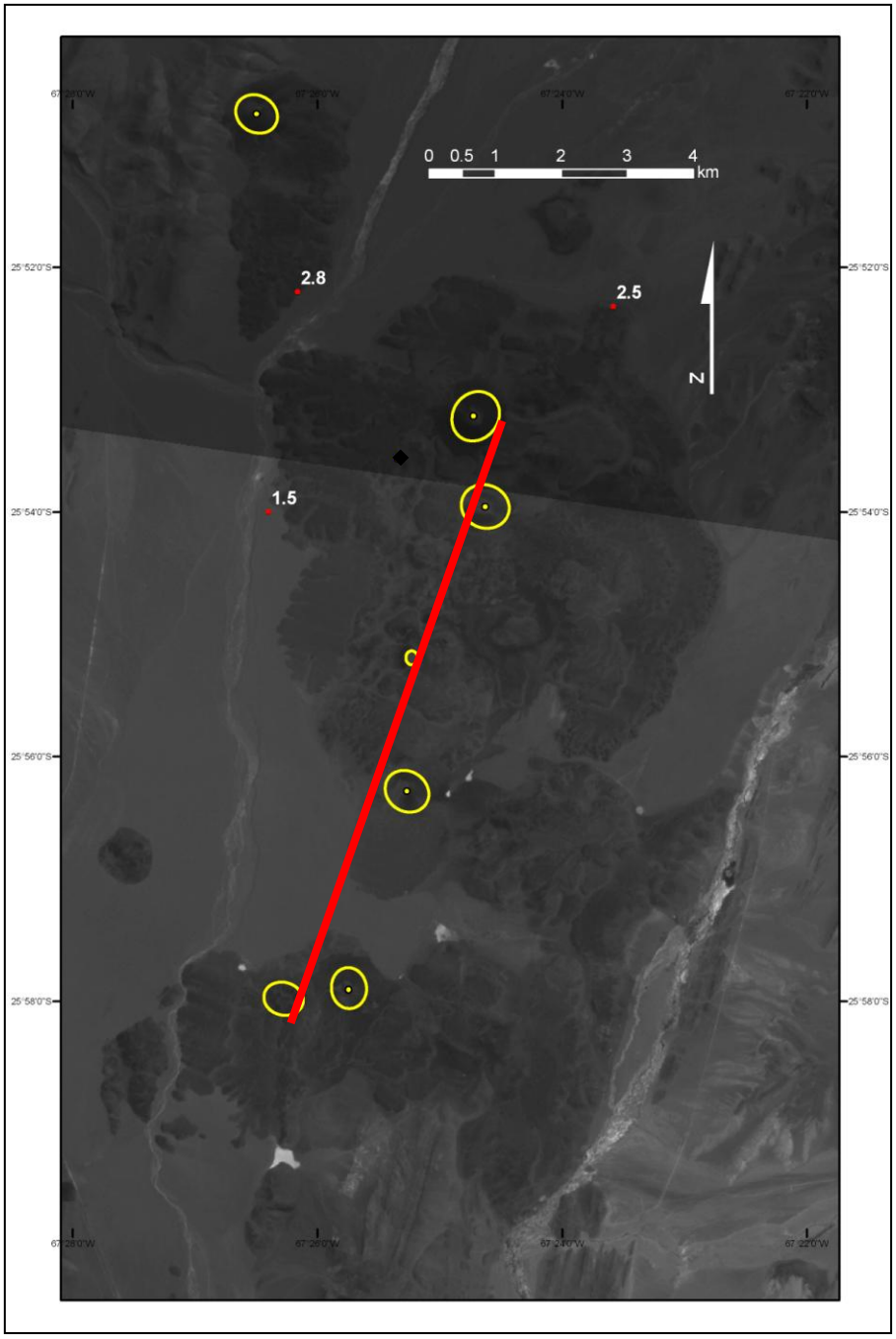

Figure 6. The Nacimientos field showing ellipses fitted to the bases of vents (yellow) and the alignment trend (red).

Jote Volcanic Field

The Jote volcanic field (figure 7.), which is situated in the southern part of the Antofagasta basin, covers roughly 50 km² and consists of nine cinder cones with associated flows. The largest of the nine cones has long and short axes of 2092.2m and 1820.2m respectively and a height of about 490m. The other cones are considerably

smaller and have long axes ranging from 1281.6 m to 627.8 m. I propose two different volcanic alignments within the field, Jote north and Jote south, based on the alignment analyses methods laid out in Paulsen and Wilson (2010).

Jote north contains four cones with an average spacing distance of 1495 m and an average long axis azimuth of 99° (107°, 60°, 124°, 103°). Note there is one cone within this proposed alignment (60°) that trends nearly perpendicular to the others. Three of the flows in the field have been dated by Risse (2008) to 3.5, 3.2, and 2.43 Ma. Three cones breached to the west and one to the NW. Three of the cones have axial ratios that are slightly elongate (>1.2 ratio long to short axes) and one is circular. The proposed alignment azimuth is 115° and the standard angular deviation of the trend of the vent long axes from 115° is 22.6. Application of the reliability assessment system for vent alignments from Paulsen and Wilson (2010) provides a grade of "C" for this alignment. This is due mostly to the high standard deviation best-fit line distance which is 139.2m for the Jote north alignment. The other parameters that factor into the grading scheme are number of vents (4), index of elongation, standard angular deviation vent long axes (22.6°), and average vent spacing distances which is not applicable for this alignment.

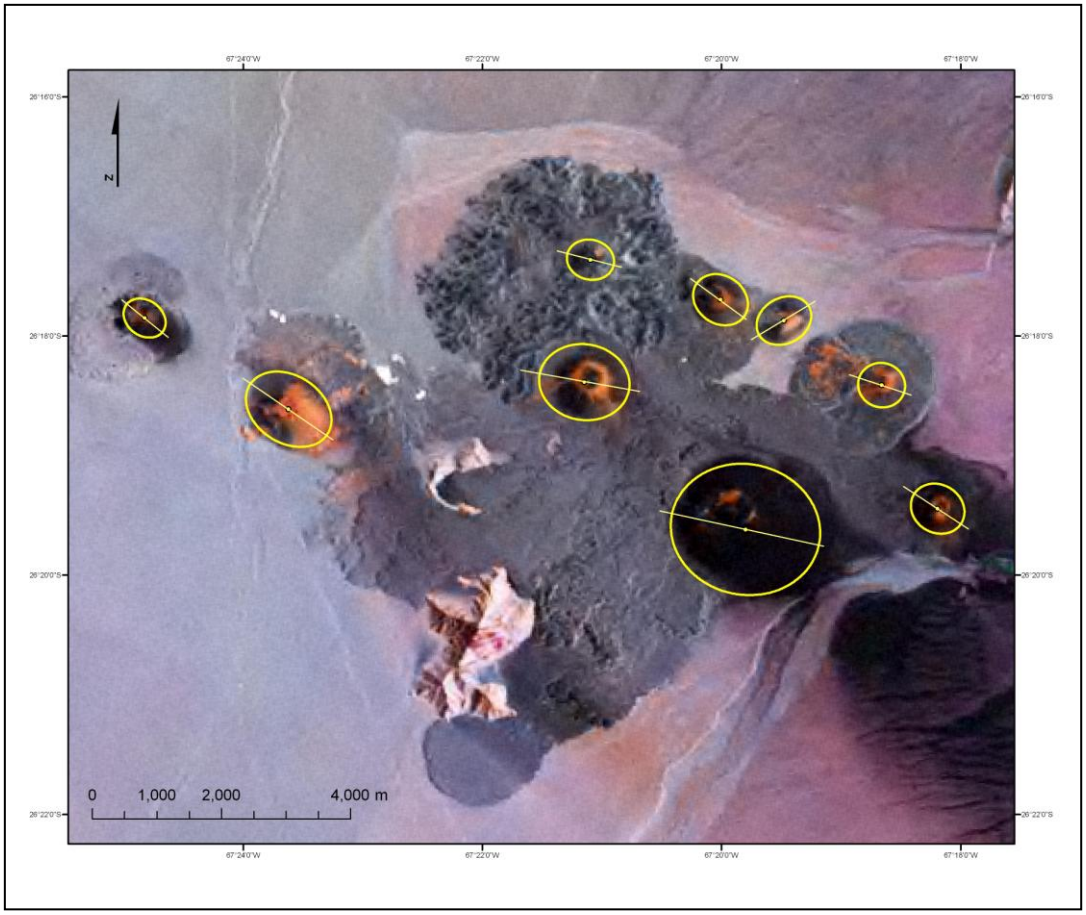

Figure 7. The Jote volcanic field contains 9 cones. This figure shows the ellipses that were fitted to each individual cone and the long axis orientation of each.

Jote south contains five cones with an average spacing distance of 2851m and an average long axis azimuth of 114° (127°, 123°, 121°, 99°, 101°). This is a relatively large field with a length of about 11.5 km. Of the five cones within the alignment, three are slightly elongate and two are circular. Four cones breached to the west and one to the north. The largest of any of the cones in the entire Jote field is part of the Jote south alignment and has a long axis trend of 101°, which is very similar to the proposed alignment trend of 104.4°. Application of the reliability assessment system for vent alignments from Paulsen and Wilson (2010) gives a grade of "D" for the Jote south alignment. Similar to the Jote north field, this is mostly due to the large standard deviation best-fit line distance (272.9m), and also to the large average vent spacing

distance. The cones within Jote south have a very low standard deviation (8.42°) of vent long axes from the trend of the best fit line, which is another of the parameters of the reliability assessment system but is over-ridden by the large standard deviation best-fit line distance.

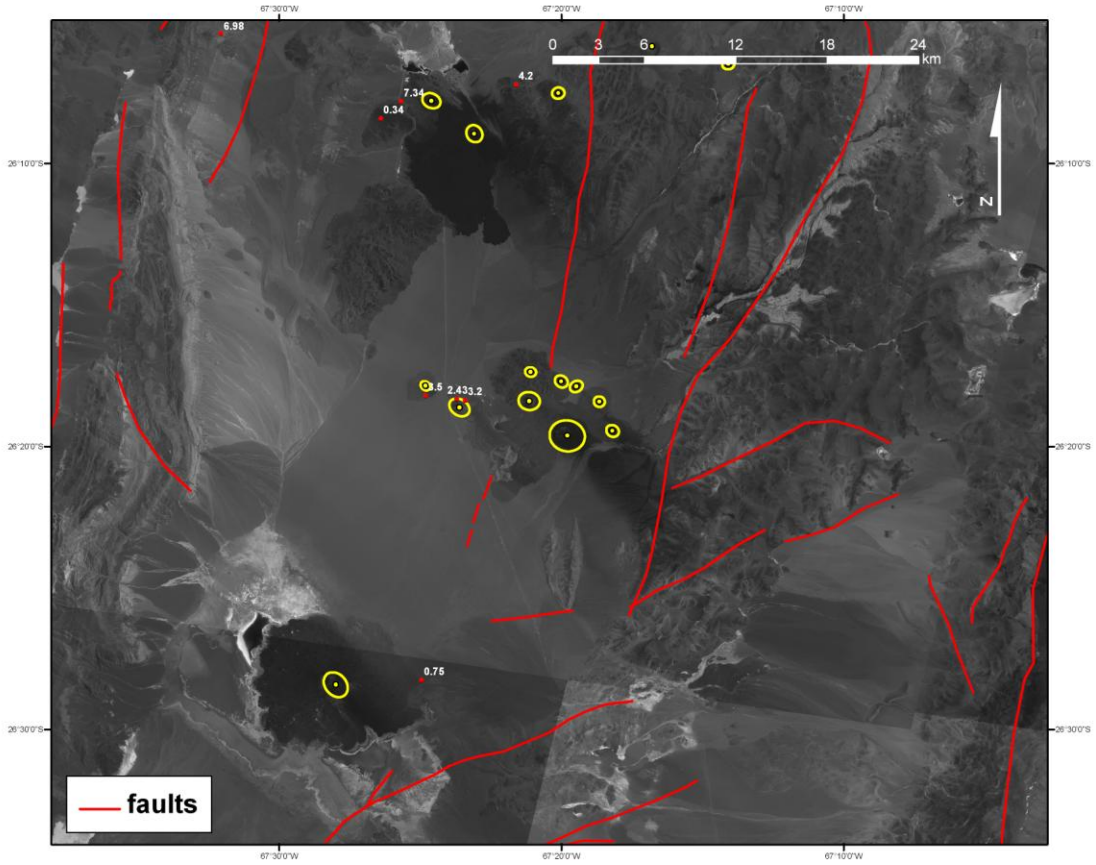

Figure 8. N-S faults shown in the area of the Jote volcanic field.

Discussion

Our data show a strong preferred NW-SE basal elongation of volcanic vents within the Puna Plateau (see rose diagram). This preferred elongation is curious in an area that is believed to have undergone a recent shift from compressional tectonics to extensional, marked by generally N-S to NE-SW trending faults of both regime types and known structure inheritance. This direction is similar to the direction of plate convergence as well as some of the large scale tectonic lineaments such as the Colama-Olcapato-El Toro, Archibarca-Galan, and Culampaja-Farallon-Negro. These lineaments

are large, orogen scale alignments of super-voluminous polygenetic volcanoes (figure 9 Showing tectonic lineaments. From Matteini et al., 2002). These lineaments represent such large scale features that their relationship with small volume monogenetic cinder cones are difficult to decipher, but and may be insignificant.

If magma was ascending through a generally N-S extensional regime in which orogen parallel thrust planes were being reactivated to accommodate extension, we would expect an overall N-S trend in both cone elongation and vent alignment. This is the case in the Nacimientos field which shows both a general N-S to NE-SW elongation and alignment of volcanic vents. Within Nacimientos, local N-S to NE-SW striking faults are parallel to cone alignment. This alignment direction is consistent with NW-SE extension. However, some cone elongation is sub-perpendicular, dominantly to the NW-SE. Thus cone elongations partially disagree with field alignment.

In contrast, the two alignments within the Jote field are clearly oriented NW-SE, suggesting the involvement of a buried structure. A NE-SW trending fault is observable as terminating into the northern part of the Jote field and has been inferred on the south side of the field. The possibility remains that a buried step-over structure between possible subsurface faulting may have provided a means for ascending magma to reach the surface. The topographic substrate is relatively flat with a subtle westerly slope of about .02, making any topographic influence negligible. The alignments obtained from these data indicate extension not recorded by the orientation of surface faults, and therefore provide crucial data for plateau wide stress analyses.

In conclusion, our data do not support a radial drip model which would produce a radial stress pattern or a multiple drip model which would produce a more complicated pattern. Our data are more supportive of a delamination or ‘peeling back’ model.

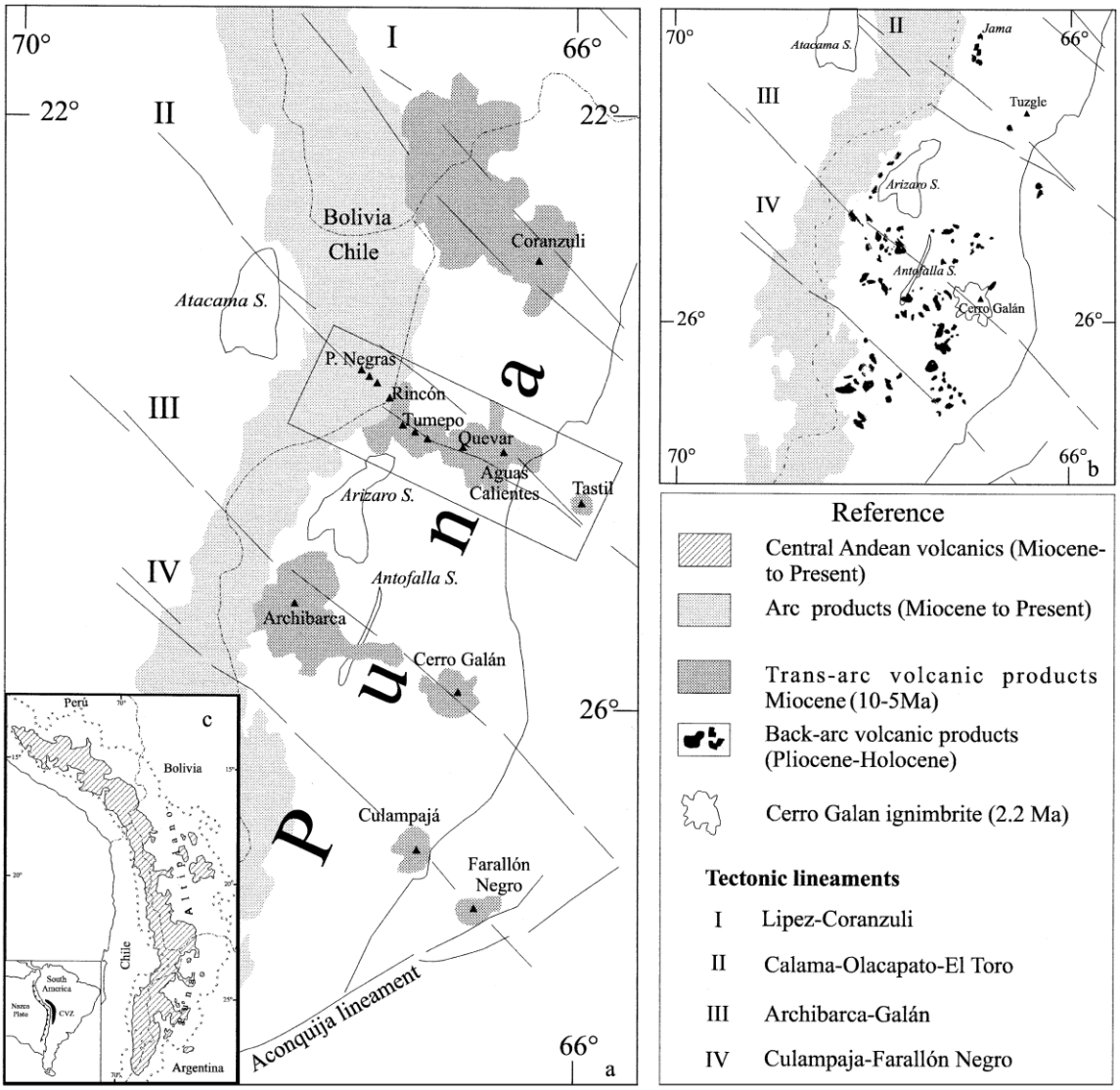

Figure 9. from Matteini et al., 2002

Table 1. Morphometric parameters of monogenetic vent alignments

Location	Rock Type	# Vents	Length (km)	# of Elongate Vents	std. dev. BF line dist. (m)	Standard Angular Deviation Vent Long Axes (°)	Avg. Vent Spacing Dist. (m)	Alignment Azimuth (°)	Avg. Vent Long Axis AZ. (°)	Reliability Assessment Grade
Naciementos	Basalt-Basaltic Andesite	7	9.36	1	161.33947	30.98036	1591.7	20.29	120.0452	C
Individual parameter grade		A		A (Cleft cone)	C	A	N/A			
Jote North	Basalt-Basaltic Andesite	4	4.47	3	139.23734	22.61186	1494.9	115.04	98.869568	C
Individual parameter grade		A		C	B	A	N/A			
Jote South	Basalt-Basaltic Andesite	5	11.487	3	272.87792	8.4233	2851	104.4	114.16084	D
Individual parameter grade		A		C	D	A	N/A			

Table 2. Reliability assessment system for vent alignments.

Reliability grade	# vents	Standard deviation best-fit line distance (m)	Index of vent elongation	Standard angular deviation vent long axes (°)	Avergae vent spacing distance (m)
A	≥4	≤125	1 cleft cone -or- 1 fissure ridge -or- 2≥1.6 -or- 1≥1.6 and 1≥1.4	≤30	No limit
	≥5	≤100	No shape data	No shape data	≤600a or ≤800b
B	≥3	≤150	1≥1.6 -or- 2≥1.4 -or- 1≥1.5 and 2≥1.2	≤35	No limit
	≥4	≤125	No shape data	No shape data	≤600a or ≤800b
C	≥2	≤175	1≥1.4 -or- 2≥1.2	≤40	No limit
	≥3	≤150	No shape data	No shape data	≤800a or ≤1000b
D	≥2	>175	1≥1.2	>40	No limit
	≥3	>150	No shape data	No shape data	>800a or >1000b

a For vents on the flanks of polygenetic volcanoes.

b For vents within platform fields.

Appendix

cone	Location	Long	Lat	XStdDist	YStdDist	Rotation (°)	long axis (m)	short axis (m)	axial ratio	Vent Shape	Breaching Direction	Age (ma)
9b	Jote north 4	-67.311	-26.306834	0.003293	0.00308	107.1883	658.6	616.8	1.067769131	circular	W ~ 270°	
8b	Jote south 1	-67.4137	-26.297481	0.003139	0.00246	126.5829	627.8	492	1.27601626	slightly elongate	various: NE, NW, SW	
7b	Jote south 2	-67.3937	-26.310196	0.006408	0.0047	122.6036	1281.6	939.2	1.364565588	slightly elongate	various: W, NE	2.43 - 3.2
6b	Jote south 5	-67.3032	-26.324054	0.003869	0.00335	121.1632	773.8	669.4	1.155960562	circular	NW ~ 300 0176	
5b	Jote north 3	-67.3246	-26.297839	0.003166	0.004	60.40192	799	633.2	1.261844599	slightly elongate	W ~ 270°	
4b	Jote north 2	-67.3335	-26.294925	0.004025	0.00334	124.3298	805	667	1.206896552	slightly elongate	NW ~ 300°	
47b	N. of Antofalla mtn.	-67.9169	-25.133041	0.004212	0.00342	94.84204	842.4	683.6	1.23229959	slightly elongate		
45b	N. of Antofalla mtn.	-67.9638	-25.245942	0.004624	0.00383	123.4544	924.8	766.2	1.206995563	slightly elongate	W ~ 280°	
44b	N. of Antofalla mtn.	-67.9694	-25.396878	0.00487	0.00417	132.4958	974	834.8	1.166746526	circular	closed	
43b	NE. of Antofalla mtn.	-67.7355	-25.419181	0.003332	0.0029	92.17574	666.4	580	1.148965517	circular	S ~ 180°	
42b	NE. of Antofalla mtn.	-67.7484	-25.418052	0.006031	0.0049	102.2529	1206.2	979.6	1.231318906	slightly elongate	closed	
41b	N. of Peinado	-68.1464	-26.480436	0.003843	0.00447	77.32394	894.8	768.6	1.16419464	circular		
40b	S. end of Salar de Antofalla	-68.1145	-26.222439	0.002905	0.00268	137.8718	581	535.6	1.08476475	circular		
3b	Jote south 3	-67.3525	-26.306422	0.006322	0.00528	99.04553	1264.4	1056.2	1.197121757	slightly elongate	W ~ 265°	
39b	E. side of Salar de Antofalla	-67.7976	-26.003592	0.003937	0.00481	80.15868	962.6	787.4	1.222504445	slightly elongate		
38b	E. side of Salar de Antofalla	-67.7451	-25.960533	0.008217	0.00531	95.63636	1643.4	1062.2	1.547166259	elongate		
37b	Naciementos	-67.4416	-25.845768	0.002946	0.00249	121.0828	589.2	498.8	1.181234964	circular	NE ~50°	2.8
36b	N. of Peinado	-68.0257	-26.420676	0.005385	0.00497	141.0182	1077	994.2	1.083283042	circular		
35b	S. of Peinado	-68.0631	-26.672553	0.002988	0.00329	43.61334	658.6	597.6	1.102074967	circular		
34b	S. Pasto Ventura	-67.3578	-26.87146	0.003412	0.00302	141.7546	682.4	604.2	1.129427342	circular		
33b	N. of Antofalla mtn.	-67.9452	-25.40245	0.003603	0.00337	107.6689	720.6	674.8	1.067871962	circular	NE ~ 25 °	
32b	N. of Antofalla mtn.	-67.9168	-25.392067	0.003092	0.00249	126.7677	618.4	497.6	1.242765273	slightly elongate	closed	
31b	N. of Antofalla mtn.	-67.9653	-25.259673	0.004978	0.00414	131.616	995.6	828.2	1.202125091	slightly elongate	NW ~ 300°	
30b	N. of Antofalla mtn.	-67.9488	-25.246702	0.003345	0.00268	110.6641	669	536.8	1.246274218	slightly elongate	closed	
29b	NE. of Antofalla mtn.	-67.7694	-25.21692	0.003672	0.00345	93.66835	734.4	690.4	1.06373117	circular	closed	
28b	NE. of Antofalla mtn.	-67.7848	-25.224679	0.004393	0.00401	94.91727	878.6	801.4	1.09633142	circular	N ~ 10°	
27b	NE. of Antofalla mtn.	-67.7776	-25.236522	0.004711	0.0041	130.8191	942.2	819.6	1.149585163	circular	SE ~ 130°	
26b	NE. of Antofalla mtn.	-67.771	-25.24816	0.005007	0.00452	94.344	1001.4	903.2	1.108724535	circular	NW ~ 320°	
1b	Carachi Pampa	-67.4667	-26.473625	0.008091	0.00621	138.4816	1618.2	1242.4	1.302479073	slightly elongate	all around	0.75
23b	Naciementos	-67.3049	-25.868105	0.003746	0.00354	125.9265	749.2	708	1.05819209	circular	S?	2.4
22b	N. Naciementos	-67.2903	-25.821133	0.003304	0.00243	112.7101	660.8	485.8	1.360230548	slightly elongate	W ~ 285°	2.48
21b	N. Naciementos	-67.2691	-25.833124	0.004309	0.00359	96.06688	861.8	718.2	1.199944305	slightly elongate	W ~ 280 °	
20b	N. Naciementos	-67.3161	-25.830688	0.003915	0.00353	156.1167	783	706	1.109065156	circular		
2b	Jote south 4	-67.33	-26.326951	0.010461	0.0091	101.4091	2092.2	1820.2	1.149434128	circular	W ~ 285°	
19b	Naciementos	-67.4118	-25.886914	0.00308	0.00352	36.69357	703.6	616	1.142207792	circular	NW ~310°	2.5
18b	Naciementos	-67.4105	-25.899263	0.003304	0.00293	110.0909	660.8	586.4	1.126875853	circular	NW ~310°	
17b	Naciementos	-67.4212	-25.938071	0.003114	0.0027	125.8195	622.8	539.6	1.154188288	circular	SW ~245°	
16b	Naciementos	-67.4291	-25.965074	0.002794	0.00239	166.1317	558.8	478.4	1.168060201	circular	W ~270°	
15b	E. of Antofagasta	-67.3353	-26.125038	0.003341	0.0037	78.91999	740	668.2	1.107452858	circular	NW ~ 330°	
14b	E. of Antofagasta	-67.2798	-26.097405	0.004518	0.0038	103.198	903.6	760.8	1.187697161	circular		

13b	E. of Antofagasta	-67.2349	-26.107842	0.003198	0.00362	78.57482	723.2	639.6	1.130706692	circular	closed	
12b	Antofagasta	-67.4102	-26.129513	0.005553	0.00425	114.0032	1110.6	849	1.308127208	slightly elongate	~ W	
11b	Antofagasta	-67.3848	-26.148945	0.005251	0.00454	146.4343	1050.2	907	1.157883131	circular	~ W	
10b	Jote north 1	-67.3516	-26.289346	0.003318	0.00277	103.5583	663.6	554.6	1.196538045	slightly elongate	N	3.5
49b	N. of Antofalla mtn.	-67.8907	-25.42239	0.005559	0.00305	111.884	1111.8	609	1.825615764	very elongate		
48b	N. of Antofalla mtn.	-67.9302	-25.398166	0.004149	0.00376	95.34109	829.8	751.8	1.103750998	circular	NW ~300°	
50b	Naciementos	-67.438	-25.966335	0.00271	0.00224	105.0517	542	447	1.212527964	slightly elongate	various	
51cleft	Naciementos	-67.4205	-25.919884	0.000954	0.00082	176.484	190.8	163	1.170552147	cleft cone		

References

Allmendinger, R.W., 1986, Tectonic development, southeastern border of the Puna Plateau, northwestern Argentine Andes: GSA Bulletin, v. 97, p. 1070-1082.

Allmendinger, R.W., Jordan, T.E., Kay, S.M., and Isacks, B.L., 1997, The evolution of the Altiplano-Puna plateau of the central Andes: Annual Review of Earth and Planetary Science, v. 25, p. 139-174.

Allmendinger, R.W., Strecker, M., Eremchuck, J.E., and Francis, P., 1989, Neotectonic deformation of the southern Puna Plateau, northwestern Argentina: Journal of South American Earth Sciences, v. 2, p. 111-130.

Beck, S.L., and Zandt, G., 2002, The nature of orogenic crust in the central Andes: Journal of Geophysical Research, 107(B10), 2230, doi: 10.1029/2000JB000124.

Carrapa, B., Schoenbohm, L., DeCelles, P., Clementz, M., Huntington, K., and Quade, J., 2009, Surface response to lithospheric delamination: an example from the Puna Plateau of NW Argentina: Geological Society of America Abstracts with Programs, v. 41, no. 7, p. X.

Coira, B., and Kay, S.M., 1993, Implications of Quaternary volcanism at Cerro Tuzgle for Crustal and Mantle evolution of the Puna Plateau, Central Andes, Argentina: Contributions to Mineralogy and Petrology, v. 113, p. 40-58.

Coira, B., Kay, S.M., and Viramonte, J., 1993, Upper Cenozoic magmatic evolution of the Argentina Puna-A model for changing subduction geometry: International Geology Review, v. 35, p. 677-720.

de Silva, S. L., 1989, Altiplano-Puna volcanic complex of the central Andes: Geology, v. 17, p. 1102-1106.

de Silva, S.L. & Francis, P.W. 1991, Volcanoes of the Central Andes: Springer Verlag, Berlin, 216.

Drew, S., Ducea, M., Schoenbohm. L., 2009, Mafic volcanism on the Puna Plateau, NW Argentina: Implications for lithospheric composition and evolution with an emphasis on lithospheric foundering. Lithosphere Vol.1, page 305-318.

Garzione, C.N., Molnar, P., Libarkin, J.C., and MacFadden, B.J., 2006, Rapid late Miocene rise of the Bolivian Altiplano: evidence for removal of the mantle lithosphere: Earth and Planetary Science Letters, v. 241, p. 543-556.

Göğüs, O.H., and Pysklywec, R.N., 2008a, Mantle lithosphere delamination driving plateau uplift and synconvergent extension in eastern Anatolia: Geology, v. 36, p. 723-726.

Göğüs, O.H., and Pysklywec, R.N., 2008b, Near-surface diagnostic of dripping or delaminating lithosphere: Journal of Geophysical Research, v. 113, B11404, doi: 10.1029/2008JB005123.

Guzmán S, R., Petrinovic I., and Brod J. A., 2006, Pleistocene mafic volcanoes in the Puna–Cordillera oriental boundary, NW-Argentina: Journal of Volcanology and Geothermal Research, v. 158, p. 51-69.

Isacks, B., 1988, Uplift of the central Andean plateau and bending of the Bolivian orocline: Journal of Geophysical Research, v. 93, p. 3211-3231.

Kay, S.M., Coira, B., and Viramonte, J., 1994, Young mafic back arc volcanic rocks as indicators of continental lithospheric delamination beneath the Argentine Puna plateau, central Andes: Journal of Geophysical Research, v. 99, p. 24,323-24,339.

Kay, S.M., Coira, B., Woerner, G., and Singer, B.S., 2008, Cerro Galan ignimbrite: Trace element, isotopic and $^{40}Ar/^{39}Ar$ age constraints on the evolution of the central Andean lithosphere, Eos Trans. AGU, 89(53), Fall Meet. Suppl., Abstract V22A-06.

Kay, S.M., Godoy, E., and Kurtz, A., 2005, episodic arc migration, crustal thickening, subduction erosion, and magmatism in the south-central Andes: GSA Bulletin, 117, 67-88.

Kay, R.W., and Kay, S.M., 1993, Delamination and delamination magmatism. Tectonophysics: v. 219, p. 177-189.

Kraemer, B., 1999, A geochemical traverse across the middle Miocene magmatic arc in the southern part of the central volcanic zone of the Andes (25°-26°30°s, 67°30^-69^w): Gerliner Geowiss. abh. A, v. 200, p. 1-174.

Kraemer, B., Adelmann, D., Alten, M., Schnurr W, B., Erpenstein, K., Fiefer, E., van den Dogaard, P., and Görler, K., 1999, Incorporation of the Paleogene foreland into the Neogene Puna Plateau: The Salar de Antofalla area, NW Argentina: Journal of South American Earth Science, p. 157-182.

Marrett, R.A., Allmendinger, R.W., Alonso, R.N., and Drake, R.E., 1994, Late Cenozoic tectonic evolution of the Puna Plateau and adjacent foreland, northwestern Argentine Andes: Journal of South American Earth Sciences, v. 7, p. 179-207.

Marrett, R.A., and Emerman, S.H., 1992, The relations between faulting and mafic magmatism in the Altiplano-Puna plateau (central Andes): Earth and Planetary Sciences Letters, v. 112, p. 53-59.

Marrett, R., and Strecker, M.R., 2000, Response of intracontinental deformation in the central Andes to late Cenozoic reorganization of South American Plate motions: Tectonics, v. 19, p. 452-467.

McKenzie, D., and Bickle, M.J., 1988, The volume and composition of melt generated by extension of the lithosphere: Journal of Petrology, v. 29, p. 625-679.

McQuarrie, N., Horton, B.K., Zandt, G., Beck, S., and Decelles, P.G., 2005, Lithospheric evolution of the Andean fold-thrust belt, Bolivia, and the origin of the central Andean Plateau: Tectonophysics, v. 399, p. 15-37.

Nakamura, K., 1977. Volcanoes as possible indicators of tectonic stress orientation—principal and proposal. Journal of Volcanology and Geothermal Research 2, 1–16.

Nakamura, K., Jacob, K.H., Davies, J.N., 1977. Volcanoes as possible indicators of tectonic stress orientation—Aleutians and Alaska. Pure and Applied Geophysics 115, 87–112.

Paulsen, T.S., Wilson, T.J., 2010. New criteria for systematic mapping and reliability assessment of monogenetic volcanic vent alignments and elongate volcanic vents for crustal stress analyses; Tectonophysics, v. 482, p. 16-28.

Risse, A., Trumbull, R.B., Coira, B., Kay, S.M., and van den Bogaard, P., 2008. $^{40}Ar/^{39}Ar$ geochronology of mafic volcanism in the back-arc region of the southern Puna plateau, Argentina: Journal of South American Earth Science, v. 26, p. 1-15.

Schoenbohm, L.M., and Strecker, M., 2009, Normal faulting along the southern margin of the Puna Plateau, Northwest Argentina: Tectonics, VOL. 28, TC5008.

Tassara, A., Goetze, H.J., Schmidt, S., and Hackney, R., 2006, Three-dimensional density model of the Nazca plate and the Andean continental margin: Journal of Geophysical Research, v. 111, p. 1-26.

Tibaldi, A., 1995. Morphology of pyroclastic cones and tectonics: Journal of Geophysics Research, v. 100, p. 24, 521-24, 535.

Zandt, G., Gilbert, H., Owens, T., Ducea, M., Saleeby, J., and Jones, C., 2004, Active foundering of a continental arc root beneath the southern Sierra Nevada in California: Nature, v. 431, p. 41-46